Inorganic Chemistry

Article

pubs.acs.org/IC

Histidine Based Fluorescence Sensor Detects Hg^{2+} in Solution, Paper Strips, and in Cells

Joydev Hatai, Suman Pal, Gregor P. Jose, and Subhajit Bandyopadhyay*

Department of Chemical Sciences, Indian Institute of Science Education and Research Kolkata, BCKV Campus PO, Mohanpur, Nadia, WB 741252, India

Supporting Information

ABSTRACT: A chemosensor having a bipodal thiocarbamate scaffold attached to histidine moieties senses Hg^{2+} with a remarkable selectivity. The binding results in a 50 nm blue shift in the fluorescence spectra and a 19-fold enhancement of the fluorescence quantum yield of the ligand. In addition to the detection of Hg^{2+} visually under UV light in solution, the chemosensor was used for fabrication of paper strips that detected Hg^{2+} in aqueous samples. The sensor was also used for imaging Hg^{2+} in adult zebrafish and in human epithelial carcinoma HeLa S3 cells.

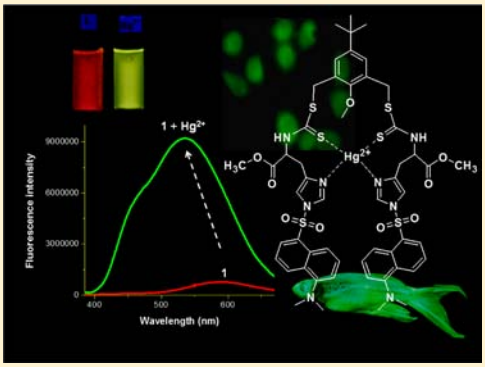

INTRODUCTION

Mercury is an important analyte because of its toxic effect in the ecosystem.[1,2] Apart from anthropogenic activities, environmental contamination by mercury occurs from volcanic eruptions, geothermal vents, and leaching of mercury from ores, such as cinnabar, into natural sources of water.[3] Depending on the environment, Hg^{2+} can be transformed to Hg^0 and also to highly toxic organomercury compounds by several strains of aerobic bacteria.[4] The metal and its compounds are bioconcentrated and biomagnified by sea creatures, and subsequently consumed by humans, giving rise to mercury poisoning. Dental amalgam is also a source of mercury toxicity.[5] Organomercury compounds can easily cross the cell membranes and the blood brain barrier impairing nefrological and neurological functions. Because of this high toxicity, the U.S.-EPA directive for the highest concentration of mercury in drinking water is 2 ppb (10 nM).[6]

Detection and quantitative determination of mercury in its most stable Hg^{2+} form has received much attention, perhaps, more than any other toxic heavy metal ions. Quantitative detection of samples containing both organomercury species and inorganic mercury is possible with several analytical methods.[7] Atomic absorption spectrometry (AAS), atomic emission, and fluorescence spectrometry, inductively coupled plasma-mass spectrometry (ICPMS), inductively coupled plasma-atomic emission spectrophotometry (ICP-AES), and electrochemical techniques (such as ion-selective potentiometry and anodic stripping voltammetry) have high sensitivity that can even reach the submicrogram to nanogram per liter range.[8] Although these methods are unparallel in terms of sensitivity, each of these techniques bear certain disadvantages.[7] The instrumentation cost of the ICPMS is high. Moreover, it suffers in terms of selectivity for different charged states of an element. AAS suffers from the non linearity of the calibration curves, particularly at higher absorbance range. Highly sensitive voltammetric methods such as the one with hanging drop mercury electrode have several disadvantages. It has a low surface area to volume ratio that causes a reduction of the plating efficiency, and the large volume yields a low concentration of metal in mercury.[9]

Although the sensitivity of fluorogenic detection is lower by several orders in magnitude, it has certain advantages because of its low cost, facile sample preparation, high selectivity, and easy detection by both visual and instrumental methods. The importance of detection of mercury ion has prompted researchers to detect it fluorogenically through a diverse range of approaches. The most popular ones are based on optical responses with small molecules having luminescent probes.[10] Often the luminescent probes are based on nanoparticles,[11] semiconductor nanocrystals,[12] polymer−oligonucleotide composites,[13] metal regulatory proteins,[14] and nucleotide conjugates such as DNAzymes,[15] DNA hydrogels,[16] and DNA-functionalized silica nanoparticles.[17] There are reports of chemodosimeters where the effect of the ion cannot be reversed.[18] The detection methodologies of these sensors rely on the changes in the fluorescence intensity and color and hence the sensing can be carried out visually with the naked eye, or with a spectrometer. Lippard[19] and later, Kim[20] have extensively reviewed optical sensors for mercury ions. Luminescence responses involve several energy or electron transfer mechanisms that have been discussed systematically in

Received: March 12, 2012
Published: September 14, 2012

dx.doi.org/10.1021/ic300530f | Inorg. Chem. 2012, 51, 10129−10135

these articles. The sensors, based on photoinduced electron transfer (PET) mechanism, exhibit enhancement of fluorescence intensity with small shifts in the emission wavelengths, whereas, pronounced signal enhancement accompanying a large blue-shift in the emission wavelength is typically observed where the addition of the ion inhibits internal charge transfer (ICT) process.[21] Many of the ICT-based mercury sensors only work with organic solvents and lack selectivity from competing metal ions.[19,22]

To date there are reports of only a few amino acid based Hg^{2+} sensors, including lysine,[23a] aspartic acid-BSA conjugate,[23b] tryptophan[23c] and methionine based.[23d] In all cases the detection of mercury occurred by appending a fluorophore directly to the amino acid. Further modification of the amino acid structure was not required. In this article, we report a histidine based turn-on fluorescence sensor for Hg^{2+}, which is unique because histidine normally has a strong affinity for Cu^{2+}.[24] We have appended histidine residues to a bipodal thiocarbamate scaffold to provide sulfur atoms as donors and alter its selectivity. Dithiocarbamates with simple amines have been used by Kamata et al. as ionophores for Hg^{2+} and Ag^{+} ions and in ion selective electrodes for heavy metals.[25] We have recently demonstrated the use of the thiocarbamate scaffold attached to a salicyl aldehyde based aryl system and coumarin fluorophores for differential detection of multiple metal ions by tuning of solvents.[26] In this case, the histidine based sensor displays a turn-on fluorescence behavior with high selectivity for mercury with a large emission shift ($\Delta\lambda$ = 50 nm, from 590 to 540 nm) and a 19-fold enhancement of the fluorescence quantum yield. The sensor works in mixed aqueous−organic media (MeOH/H_2O, 80:20, v/v with 1% acetonitrile as a cosolvent, buffered at pH 7.0 with HEPES) at 25 °C and is highly selective for Hg^{2+} ions, which is remarkable given that mercury sensors are commonly known to respond to other ions along with Hg^{2+}, namely, Ag^{+}, Cd^{2+}, Fe^{2+}, and Pb^{2+}.[27] Interestingly, Cu^{2+} ion responded to the sensor with a quenching of the fluorescence. Additionally, fabrication of a simple dip-strip that works in real time scale with aqueous samples is always desirable for convenient in-field detection of Hg^{2+} contaminated samples. Paper based strips were fabricated with the chemosensor that were able to detect Hg^{2+} in aqueous solutions. The probe was also successfully used for detection of mercury in adult zebrafish samples and in carcinoma cells.

The bipodal chemosensor **1** (Figure 1A) consists of two dithiocarbamate moieties appended to histidine units bearing dansyl fluorophores. The central aryl unit, which under our excitation conditions is nonfluorescent, serves as the linker. The synthetic route for the sensor **1** is shown in Scheme 1. The key step of the synthesis was performed under aqueous conditions where the methyl ester of histidine **3**[28] upon treatment with carbon disulfide and the bromomethyl compound **2**[29] in dioxane−water (1:4, v/v) mixture afforded the thiocarbamate compound **4** in a single step. Dansylation of compound **4** in presence of 2 equiv of triethylamine in dry dichloromethane afforded **1** in 45% yields. The structure of **1** was confirmed by ^{1}H and ^{13}C NMR, IR, and MS data.

The metal affinity of chemosensor **1** toward a variety of cations: Cr^{3+}, Mn^{2+}, Fe^{2+}, Fe^{3+}, Co^{2+}, Hg^{2+}, Ni^{2+}, Cu^{2+}, Zn^{2+}, Pb^{2+}, Ag^{+}, Al^{3+}, Ba^{2+}, Ca^{2+}, Cd^{2+}, K^{+}, Na^{+}, Li^{+} was investigated by absorption and fluorescence spectroscopy in mixed aqueous−organic solvent conditions mentioned earlier.

Compound **1** in the absence of any metal ion showed an absorption band centered at 373 nm and at 260 nm (Figure 2).

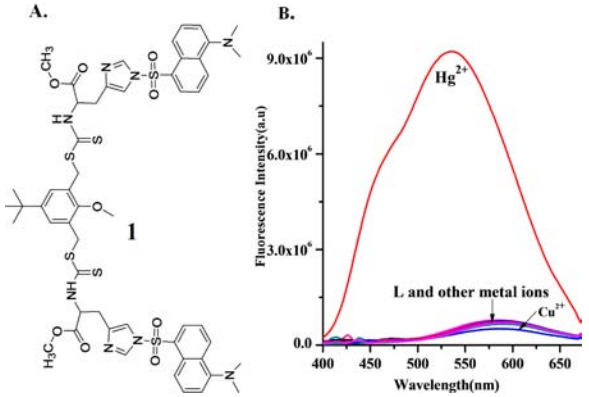

Figure 1. (A) Structure of **1**. (B) Fluorescence spectra (λ_{ex} = 340 nm, excitation and emission slit widths = 4.5 nm) of **1** (10 μM) and addition of different metal salts (60 μM) in mixed solvent media (MeOH/H_2O, 80:20, v/v with 1% acetonitrile as a cosolvent, buffered with HEPES) at pH 7.0 at 25 °C.

Scheme 1. Synthesis of the Bipodal Chemosensor 1

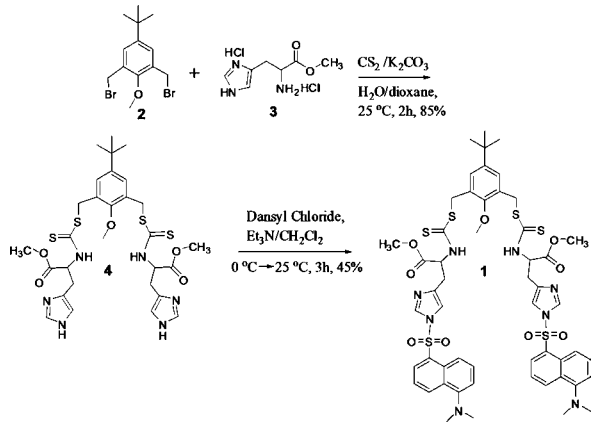

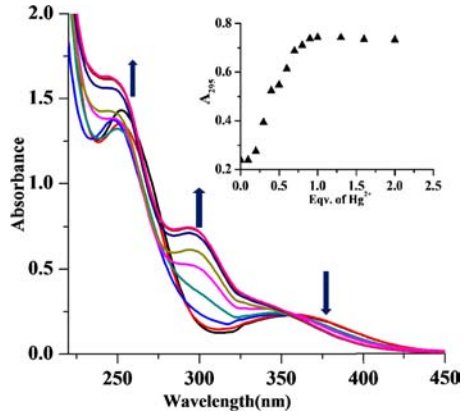

Figure 2. Change in the absorption spectra of chemosensor **1** (10 μM) with increasing concentration of $Hg(NO_3)_2$ (0 to 30 μM) in mixed solvent media (MeOH/H_2O, 80:20, v/v with 1% acetonitrile as a cosolvent, buffered with 1 mM HEPES) at pH 7.0 at 25 °C (Inset: Hg^{2+} titration profile at 295 nm).

On addition of Hg^{2+}, the absorption band at 373 nm diminished, and a new band at 295 nm was observed. The change in the absorption spectra was significant up to addition of 1 equiv of Hg^{2+} (inset, Figure 2). This indicates that the binding of Hg^{2+} with **1** takes place in a 1:1 ratio.

dx.doi.org/10.1021/ic300530f | Inorg. Chem. 2012, 51, 10129−10135

The fluorescence spectrum (λ_{ex} at 340 nm, excitation and emission slit widths = 4.5 nm) of **1** (10 μM) displays with a weak fluorescence band at 590 nm (quantum yield, Φ = 0.022) in mixed solvent media ($MeOH/H_2O$, 80:20, v/v with 1% acetonitrile as a cosolvent, buffered at pH 7.0 with 1 mM HEPES) at 25 °C. Under the same conditions, addition of Hg^{2+} (0−40 μM) to ligand (10 μM), afforded a 17-fold enhancement of the fluorescence intensity and 19-fold enhancement of quantum yield (Φ = 0.402). A large blue shift of 50 nm of the fluorescence band was also observed (Figure 1B).

The visual appearance of the samples under 366 nm light changed from dark orange to greenish-yellow (Figure 4A). The fluorescence response of chemosensor **1** (10 μM) was also tested with different metal ions such as Cr^{3+}, Mn^{2+}, Fe^{2+}, Fe^{3+}, Co^{2+}, Ba^{2+}, Ni^{2+}, Cu^{2+}, Zn^{2+}, Pb^{2+}, Ag^{+}, Ca^{2+}, Cd^{2+}, K^{+}, Na^{+}, Li^{+}, and Al^{3+} (Figure 1B). While no significant change of fluorescence emission was observed in the presence of these metal ions (60 μM), Cu^{2+} displayed a quenching effect with no shift of the fluorescence band. The fluorescence turn-on with probe **1** is therefore highly specific toward Hg^{2+}.

Additionally, the observed fluorescence response (Supporting Information, Figure S1) of chemosensor **1** to various metal ions indicates that **1** can be employed for detection of Hg^{2+} ion by simple visual inspection at this concentration range. For quantitative investigation of **1**·Hg^{2+} binding, fluorescence titration was performed by varying the concentration of Hg^{2+} to a fixed amount of **1** (10 μM) (Figure 3A). The plot of

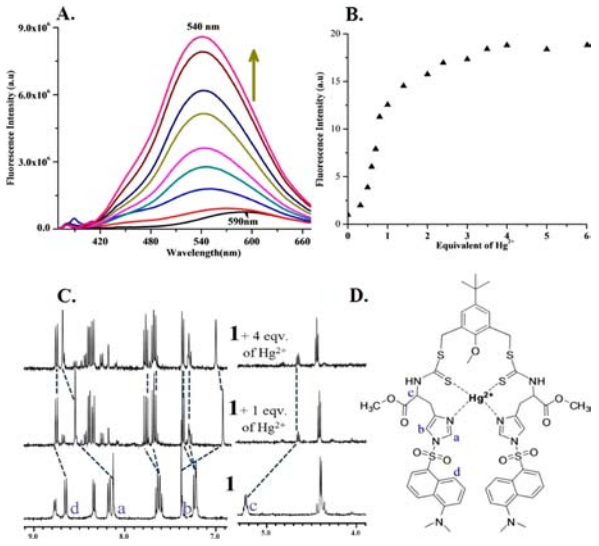

Figure 3. (A) Enhancement of fluorescence intensity (λ_{ex} at 340 nm, excitation and emission slit widths of 4.5 nm) of **1** (10 μM) with addition of Hg^{2+} (0−60 μM) in mixed solvent media ($MeOH/H_2O$, 80:20, v/v with 1% acetonitrile as a cosolvent, buffered with HEPES at pH 7.0) at 25 °C. (B) Enhancement of fluorescence intensity with addition of 0−6 equiv of Hg^{2+}. (C) ^1H NMR spectra of **1** (1×10^{-3} M) with Hg^{2+} in CD_3CN at 25 °C. (D) Putative binding mode of **1** with Hg^{2+} (see text).

fluorescence intensity of **1** at 540 nm against the added [Hg^{2+}] revealed that the fluorescence intensity increased up to addition of 1 equiv of Hg^{2+} (Figure 3B) and reached a saturation at about 4 equiv of the metal ion. A 1:1 association was established from the Job's plot experiment (Supporting Information, Figure S2). From the titration data, the binding constant was found to be 1.25 (±0.4) × 10^6 M^{-1} (Figure 5B).

A peak at m/z at 1346 in electrospray ionization mass spectrometry corresponding to one Hg^{2+} ions associating with one molecule of **1** under these conditions further supported the binding stoichiometry (Supporting Information, Figure S6B).

To test the practical applications of chemosensor **1** as a Hg^{2+} selective fluorescence sensor, competition experiments were carried out to investigate the effect of other coexisting cations with Hg^{2+} in the presence of chemosensor **1**. The emission spectra containing **1** (10 μM) and Cr^{3+}, Mn^{2+}, Fe^{2+}, Fe^{3+}, Ba^{2+}, Co^{2+}, Ni^{2+}, Zn^{2+}, Pb^{2+}, Ag^{+}, Ca^{2+}, Cd^{2+}, K^{+}, Na^{+}, Li^{+}, and Al^{3+} (60 μM) followed by addition of Hg^{2+} (40 μM) were recorded. As shown in the Figure 4C, no significant variation of fluorescence intensity was observed with other metal ions except for copper. The enhancement of fluorescence was affected significantly on addition of Hg^{2+} in presence of Cu^{2+}, and under the given conditions the enhancement was only about 40% compared to the ones without it (last bar, Figure 4C).

To elucidate the binding mode of chemosensor **1** with Hg^{2+}, an ^1H NMR spectroscopic titration experiment was performed by addition of Hg^{2+} to a CD_3CN solution of **1** (1×10^{-3} M) (Figure 3C). The protons attached to the chiral carbon shifted upfield (δ 5.23 to 4.64), indicating its proximity to the coordination site involving the thiocarbamate unit. The characteristic signal corresponding to the imidazole 2-H experienced a significant downfield shift (δ 8.13 to 8.64), indicating coordination to Hg^{2+}. The imidazole 5-H shifted upfield (δ 7.48 to 6.99). As a result of the histidine coordination, the charge transfer from the sulphonamide nitrogen to the naphthyl ring of the dansyl is reduced. This is supported in the downfield shift of the naphthalene protons. The −OMe protons had a very little upfield shift (<0.05 ppm) probably because of its out of the place orientation toward the shielding zone of the central aryl ring to avoid steric interaction with the metal ion. Taking these results into account, we propose a putative binding mode of Hg^{2+} with the ligand **1** as shown in Figure 3D.

Thus, it may be possible that in the absence of any mercury ion the weak emission intensity of the free chemosensor **1** is due to the flexibility and rotation of the imidazole ring attached to the dansyl fluorophore. This, in turn, causes an efficient ICT process from the imidazole nitrogen to the dansyl unit.[30] Coordination of Hg^{2+} restricts the ICT process and results in fluorescence enhancement. An alternate possibility is that the ligand is not fully solvated because of its hydrophobic nature. This might give rise to stacking of the chromophores causing formation of excimers, and thus quenching the probe's luminescence. Coordination of Hg^{2+} results in a positively charged complex that has a better solubility. Consequently, this circumvents the stacking and excimer formation resulting in fluorescence enhancement. This mechanism was recently observed by Fahrni with a fluorescent probe for Cu(I).[31]

To check the reversibility of the chemosensor **1**, three metal ion chelators: EDTA, *N,N,N′,N′-tetrakis*(2-pyridylmethyl)-ethylenediamine (TPEN),[32] and 8-hydroxyquinoline (100 μM each) were added separately to three different solutions containing **1** (10 μM) and $Hg(NO_3)_2$ (40 μM, corresponding to the saturation of fluorescence intensity) in $MeOH/H_2O$ (80:20, v/v with 1% acetonitrile as a cosolvent, buffered with HEPES at pH 7.0) at 25 °C. The recorded fluorescence spectra revealed that TPEN successfully decomplexed the metal ion from **1** and activated the enhanced fluorescence caused by the addition of Hg^{2+}. 8-Hydroxyquinoline was less effective at low

dx.doi.org/10.1021/ic300530f | *Inorg. Chem.* 2012, 51, 10129−10135

concentration in reverting the fluorescence turn-on; however, at a much higher concentrations (100 mM), it was able to decomplex the Hg^{2+}. EDTA minimally affected the fluorescence spectra (Supporting Information, Figure S4).

Although there are a large number of reports of Hg^{2+} sensors, simple and effective detection of the ion still remains a challenge. Encouraged by the positive results of our sensor to detect Hg^{2+}, we fabricated a simple paper strip that could detect Hg^{2+}.[33] The operation principle of our paper based strip is given in Supporting Information, Figure S3. Whatmann 1 filter papers of the dimension 5 cm ×0.75 cm was coated with a solution of **1** in acetonitrile at a height of 1 cm from the bottom of the strip (sensor zone, see Supporting Information, Figure S3) and was air-dried for one day. The strips were dipped directly into aqueous solutions containing Hg^{2+}. The Hg^{2+} was carried upward by a capillary action and the complex that formed in the sensor zone was carried to the detection zone by the solvent. After the solvent front reached a certain height, the strip was taken out, dried with a blow-drier, and the paper was held under 366 nm fluorescent light. In presence of Hg^{2+}, we envision that sensor **1** formed complex with Hg^{2+} that has a higher solubility in water compared to the hydrophobic ligand. Consequently, it moved further up in the detection zone displaying a bluish green fluorescence (Figure 4B). In the absence of mercury, such coloration was not detected in the detection zone. With this method, up to 10 μM concentration of Hg^{2+} was visually detected with the naked eye. With lower concentrations, the changes were visually less discernible. We are working on the improvement of the probe to achieve better detection limits.

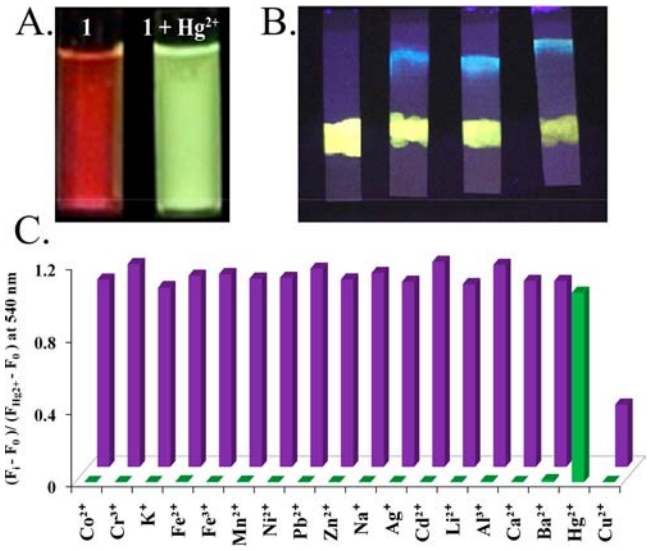

Figure 4. (A) Fluorescence images under 366 nm UV-light. (B) Photographs of the paper strip based sensing with $HgNO_3$ solutions *(left to right):* no Hg^{2+}, 10 μM, 100 μM, and 1 mM Hg^{2+} in aqueous medium buffered at pH 7.0 with HEPES (1 mM) at 25 °C. (C). *Green bars:* Changes in fluorescence intensity (λ_{ex} at 340 nm, excitation and emission slit widths of 4.5 nm) of the **1** (10 μM) upon addition of various metal salts (60 μM). *Violet bars:* Restoration of fluorescence (at same λ_{ex} and slit-widths) of **1** (10 μM) toward Hg^{2+} (40 μM) in the presence of competitive cations (60 μM) in mixed solvent media ($MeOH/H_2O$, 80:20, v/v with 1% acetonitrile as a cosolvent, buffered at pH 7.0 with 1 mM HEPES) at 25 °C.

The maximum fluorescence response of **1** was observed between pH 5.5 to 8.0 (Figure 5A), indicating that our sensor can be used at a biologically relevant pH.

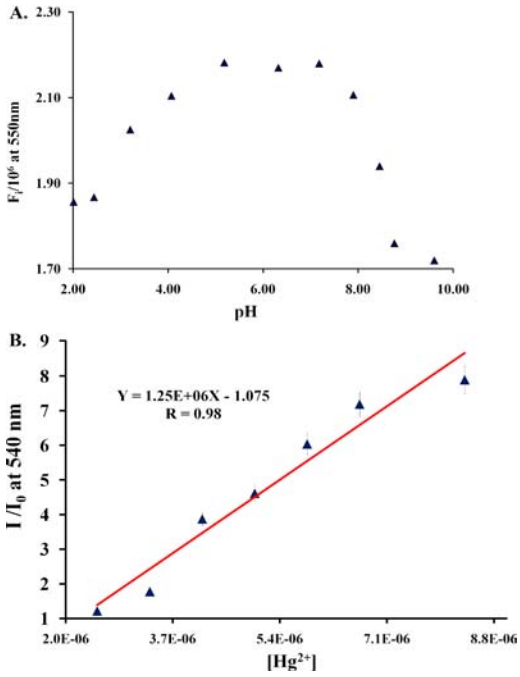

Figure 5. (A) Change in the fluorescence intensity of the emission band at 550 nm of the chemosensor **1** at different pH. (B) Benesi–Hildebrand plot for the determination of binding constant of Hg^{2+} with chemosensor **1** in mixed solvent media ($MeOH/H_2O$, 80:20, v/v with 1% acetonitrile as a cosolvent, buffered with 1 mM HEPES at pH 7.0) at 25 °C.

In solution phase ($MeOH/H_2O$, 80:20, v/v with 1% acetonitrile as a cosolvent, buffered with 1 mM HEPES at pH 7.0), the analytical detection limit[34] of Hg^{2+} with **1** was found to be 1.03×10^{-7} M (0.02 ppm) (Supporting Information, Figure S5). This value is 10 times higher than the acceptable value mandated by the U.S.-EPA for the concentration of mercury in drinking water.[6] However, the sensor can be useful in detecting inorganic mercury in samples of biological products, drugs, fish, and also in samples where regulations for mercury are less stringent.[35] The U.S. FDA has enlisted a large number of drugs and biological products such as nasal spray and ophthalmic solutions, where the concentration of inorganic mercury is allowed at the ppm level or more.[36] Probe **1** can also be used to detect mercury in certain fish when the levels are above the detection limit.[37]

Chemosensor **1** was used for the imaging of Hg^{2+} ion in cells with a fluorescence imaging experiment using an epifluorescence microscope. Human epithelial carcinoma cells, HeLa S3, were cultured in Dulbecco's Modified Eagle's Medium (DMEM), supplemented with 10% fetal bovine serum (FBS), 100 units/mL penicillin, and 100 μg/mL streptomycin, at 37 °C and 5% CO_2. Cells (0.4×10^6 per mL) were plated on 12 mm coverslips and were allowed to adhere for 24 h. The culture cells were exposed to $Hg(NO_3)_2$ (10 μM) in DMEM for 1 h at 37 °C. Immediately, before the experiments, the cells were washed twice with PBS to remove the remaining Hg^{2+} ions, and incubated with **1** (10 μM in DMSO) in PBS for 10 min at 25 °C; followed by washing the cells using PBS to remove residual dye from the cells. The series of fluororescence images revealed

marked differences in brightness of the Hg^{2+} strained cells compared to the controls (Figure 6). The fluorescence image of

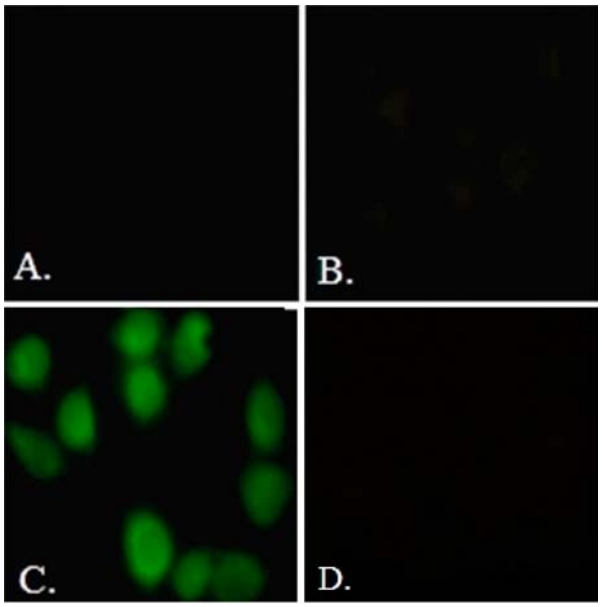

Figure 6. Fluorescence microscope images of HeLa S3. (A) Only cells. (B) Cells loaded with **1** (10 μM). (C) Cell incubated with Hg^{2+} (10 μM, 1 h, 37 °C) exposed to **1** (10 μM) for 10 min. (D) Cells stained with **1** and Hg^{2+} and subsequently treated with TPEN (100 μM) for 20 min.

HeLa S3 loaded with **1** (10 μM) under the same conditions showed weak intracellular fluorescence (Figure 6B). In contrast, cells treated with Hg^{2+} and **1** displayed vivid intracellular fluorescence (Figure 6C). To ensure that the fluorescence turn-on was due to the coordination of mercury and not some artifact or photoactivation of the probe, the stained cells were exposed to an excess (10 equiv) of metal-ion chelator *N,N,N′,N′-tetrakis*(2-pyridylmethyl)ethylenediamine (TPEN) in DMEM medium for 30 min,[32] followed by washing with PBS. On addition of the membrane permeable Hg-chelator, a gradual decrease in the fluorescence intensity was observed (Figure 6D). These results demonstrate that **1** can be used to detect intracellular Hg^{2+}.

To find out whether sensor **1** can be used for visual detection of mercury in fish, a series of experiments was carried out with adult zebrafish. The adult fishes with a mean length of 3 cm were treated with aqueous $Hg(NO_3)_2$ (10 μM) for 30 min, washed with PBS to remove any Hg^{2+} adhering to the surface, and were subsequently treated with a solution of sensor **1** (10 μM in DMSO) for 20 min, washed with PBS and observed under 366 nm light. The visual images taken with a digital camera (Figure 7) shows striking differences of the samples compared to the controls. The control zebrafish (control A) and the fish in the presence of Hg^{2+} (control B) were faintly illuminated (Figure 7A and 7B). In contrast, the fish exposed only to dye **1** displayed an orange color (Figure 7C) akin to the color of the dye under 366 nm light (Figure 4A). In certain parts of the fish: the abdomen, fins, and head, the accumulation of the color was higher compared to that in the body. In the fish exposed to both the dye and Hg^{2+}, a vividly illuminated greenish color was observed (Figure 7D). The reversibility of the green luminescence was slow even with an excess of TPEN (100 μM).

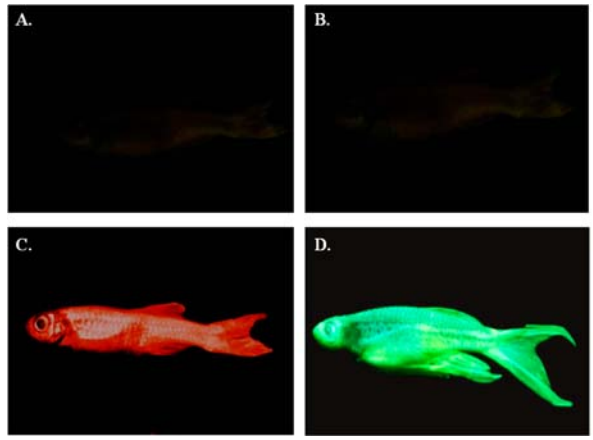

Figure 7. Images of full grown zebrafish under 366 nm light. (A) Only fish. (B) Fish incubated with $Hg(NO_3)_2$ (10 μM). (C) Fish stained with **1** (10 μM in DMSO) for 20 min. (D) Fish incubated with Hg^{2+} (10 μM) (10 min) and subsequently stained with **1** (20 min).

In conclusion, we have reported a chemosensor that senses Hg^{2+} with a large blue shift and a 19-fold enhancement of the fluorescence quantum yield in mixed aqueous−organic solvent. The sensor displayed a high selectivity for mercury ions. This selectivity of **1** inspired us to fabricate paper strips for detection of Hg^{2+} which were successful in detecting the ion in the aqueous media. The sensor also detected Hg^{2+} in fish and human epithelial carcinoma cells. The analytical detection limit of the sensor is 20 ppb, which is higher than the US-EPA mandated limit for mercury in drinking water. Development of the scaffold with improved sensitivity and better water solubility is under progress.

EXPERIMENTAL SECTION

General Information. Structures of the compounds were determined by nuclear magnetic resonance (NMR).^{1}H and ^{13}C NMR spectra were recorded on a 400 MHz Jeol and 500 MHz Bruker respectively. Chemical shifts are reported in δ values relative to an internal reference of tetramethylsilane (TMS) or the solvent peak for ^{1}H NMR and the solvent peak for ^{13}C NMR. IR data were obtained with a Bruker-Optics-Alpha-T spectrophotometer. Mass spectrometry data were obtained from an Acquity Ultra Performance LC. Fluorescence imaging experiments were carried out using an Olympus IX 51 inverted microscope with UV excitation. pH data were recorded with a Sartorius Basic Meter PB-11 calibrated at pH 4, 7, and 10. Solvents used were purified and dried by standard methods. Reactions were monitored by thin layer chromatography using Merck plates (TLC Silica Gel 60 F_{254}). Developed TLC plates were visualized with UV light. Silica gel (100−200 mesh, Merck) was used for column chromatography. Yields indicate the chromatographically and spectroscopically pure compounds, except as otherwise indicated. The solvents for the spectroscopy experiments were of the spectroscopic grades and were free from any fluorescent impurities. Double distilled water was used for the experiments. The solutions of metal ions were prepared with $Al(NO_3)_3{\cdot}9H_2O$, $LiClO_4{\cdot}3H_2O$, $NaClO_4$, $KClO_4$, $Ba(NO_3)_2{\cdot}4H_2O$, $Mn(ClO_4)_2$, $Fe(ClO_4)_2{\cdot}xH_2O$, $Fe(ClO_4)_3{\cdot}xH_2O$, $Co(ClO_4)_2{\cdot}6H_2O$, $Cr(ClO_4)_3{\cdot}6H_2O$, $Cd(NO_3)_2$, $AgNO_3$, $Hg(NO_3)_2$, $Pb(ClO_4)_2$, $Ca(ClO_4)_2{\cdot}4H_2O$, $Cu(ClO_4)_2.6H_2O$, $Ni(ClO_4)$, and $Zn(ClO_4)_2{\cdot}6H_2O$ for the respective metal ions.

Synthesis. The dibromo compound **2** and the histidine methyl ester **3** were prepared following the reported methods.[26,27] The spectral and physical data were consistent with those reported.

2-{5-tert-Butyl-3-[2-(1H-imidazol-4-yl)-1-methoxycarbonyl-ethylthiocarbamoylsulfanylmethyl]-2-methoxy-benzylsulfanylthiocarbonylamino}-3-(1H-imidazol-4-yl)-propionic Acid Methyl Ester (4). The dihydrochloride salt of **3** (0.86 g, 3.6 mmol) and K_2CO_3 (1.38 g,

dx.doi.org/10.1021/ic300530f | *Inorg. Chem.* 2012, 51, 10129−10135

10 mmol) in dioxane/water (1:4) (20 mL) was stirred for 5 min at 0 °C. To it carbon disulfide (2.72 g, 9.05 mL, 36 mmol) was added, and it was stirred for another 10 min. Compound **2** (0.50 g, 1.4 mmol) dissolved in dioxane (15 mL) was added dropwise to the reaction mixture over a period of 10 min. The solution was warmed to room temperature and stirred for 2 h until the spot for the starting materials completely disappeared on the TLC plate. The solution was concentrated under reduced pressure. The solid residue was extracted in methylene chloride (20 mL) and washed with water. The organic layer was dried over anhydrous Na_2SO_4 and volatiles were removed under reduced pressure. The residue on chromatography with methylene chloride/acetonitrile, (9:1, v/v) yielded 0.80 g (85%) of compound **4** as a white foamy substance. ^{1}H NMR (500 MHz, $CDCl_3$) δ 9.22 (b, 2H, ArNH), 7.49 (s, 2H, imid-2-H), 7.35 (s, 2H, ArH), 6.75 (s, 2H, imid-5-H), 5.43 (t, J = 5 Hz, 2H, −CHCO2Me), 4.48 (s, 4H, −CH2S), 3.83 (s, 3H, -OCH3), 3.69 (s, 6H,-CO2CH3), 3.24 (t, J = 5.0 Hz, 4H, −CH2CH), 1.24 (s, 9H, t-Bu); 13C NMR (500 MHz, CDCl3) δ 198.01, 170.01, 154.02, 147.76, 135.29, 133.93, 128.60, 127.98, 115.48, 62.40, 58.99, 52.57, 34.69, 34.34, 31.20, 28.47; FT−IR (KBr, cm-1) 3221, 2954, 1738, 1483, 1362. ESI-MS cal. for $C_{29}H_{38}N_6O_5S_4H^+$, 679.18, found 679.09

Chemosensor **1**. Dansyl chloride (0.076 g, 0.29 mmol) in methylene chloride (5 mL) was added dropwise to a solution of **4** (0.10 g, 0.146 mmol) in methylene chloride (5 mL) and triethylamine (0.04 mL, 0.29 mmol) at 0 °C. After stirring for 4 h at room temperature the reaction mixture was extracted with methylene chloride (15 mL) and washed with distilled water (15 mL × 2). The organic phase was dried over anhydrous Na_2SO_4 and concentrated under reduced pressure. The residue on chromatography with methylene chloride/ethyl acetate (9:1, v/v) yielded 0.07 g (45%) of compound **1** as a fluorescent yellowish foam. ^{1}H NMR (500 MHz, $CDCl_3$) δ 8.64 (d, J = 10 Hz, 2H, ArH), 8.57 (d, J = 8 Hz, 2H, ArH), 8.29 (d, J = 7.5 Hz, 2H, ArH), 8.19 (d, J = 8.5 Hz, 2H, ArH), 8.00 (s, 2H, imid-2-H), 7.58 (q, J = 8 Hz, 2H, ArH) 7.33 (s, 2H, imid-5-H),7.18 (d, J = 7.5 Hz, 2H, ArH), 7.06 (s, 2H, PhH), 5.44 (td, J = 5 Hz, 2H, $-CHCO_2Me$), 4.49 (s, 2H, $-CH_2S$), 4.47 (s, 2H, $-CH_2S$), 3.81 (s, 3H, $-OCH_3$), 3.48 (s, 6H, $-CO_2CH_3$), 3.12 (d, J = 5.0 Hz, 4H,-CH_2CH), 2.85 (s, 12H, $-NCH_3$), 1.23 (s, 9H, *t*-Bu). ^{13}C NMR (500 MHz, $CDCl_3$) δ 198.20, 170.24, 154.35, 152.35, 147.55, 138.93, 136.73, 133.20, 132.58, 130.38, 129.84, 128.29, 127.96, 123.18, 117.16, 115.87, 115.22, 67.02, 62.44, 58.11, 52.29, 45.29, 34.68, 34.32, 31.21, 28.92. FT−IR (KBr, cm^{-1}) 3284, 2950, 1743, 1611, 1480, 1173, 1076. ESI-MS Calc.for C_{53} $H_{60}N_8O_9S_6H^+$, 1145.28, found 1145.27

UV−vis Absorption Spectroscopy. UV−visible spectra were recorded on a Hitachi U-4100 spectrophotometer. Absorption spectra were recorded with 10 μM of chemosensor **1** and various concentrations of $Hg(NO_3)_2$ (0 to 30 μM) in mixed solvent media ($MeOH/H_2O$, 80:20, v/v with 1% acetonitrile as a cosolvent, buffered with HEPES at pH 7.0) at 25 °C. Job's plot was generated from the absorption data at a total concentration of 100 μM of $Hg(NO_3)_2$ and **1** in mixed solvent media ($MeOH/H_2O$, 80:20, v/v with 1% acetonitrile as a cosolvent, buffered at pH 7.0 with HEPES) at 25 °C, from the absorption data at 346 nm.

Fluorescence Spectroscopy. Fluorescence measurements were carried out on a Horiba Jobin Yvon (Fluoromax-3). Quartz cuvettes (Starna, 3.5 mL volume) with a path length of 10 mm were used for all fluorescence measurements. Fluorescence data was recorded in mixed solvent media ($MeOH/H_2O$, 80:20, v/v with 1% acetonitrile as a cosolvent, buffered at pH 7.0 with 1 mM HEPES) at 25 °C. Excitation was performed at 340 nm with all excitation and emission slit widths at 4.5 nm unless otherwise indicated. Quantum yield data reported here were measured relative to fluorescein in 0.1 N NaOH (Φ = 0.95).[10d] The integration of the emission spectra were obtained from the Fluoromax-3 instrument directly.

■ ASSOCIATED CONTENT

Ⓢ Supporting Information

Detailed characterization of the compound **1** along with the intermediates, and additional spectroscopic details are provided. This material is available free of charge via the Internet at http://pubs.acs.org.

■ AUTHOR INFORMATION

Corresponding Author

*E-mail: sb1@iiserkol.ac.in.

Notes

The authors declare no competing financial interest.

■ ACKNOWLEDGMENTS

The authors gratefully acknowledge two anonymous reviewers for their constructive feedback and helpful suggestions, Prof. Tapas K. Sengupta for his help with the cell imaging experiments, and Dr. Anuradha Bhat for providing the zebrafish samples. This work is funded by DST (SR/S1/OC-26/2010). J.H. thanks CSIR for a Senior Research Fellowship.

■ ABBREVIATIONS

PBS, Phosphate buffered saline; TLC, thin layer chromatography; HEPES, 4-(2-hydroxyethyl)-1-piperazineethanesulfonic acid

■ REFERENCES

(1) Harris, H. H.; Pickering, I. J.; George, G. N. *Science* **2003**, *301*, 1203.

(2) Mercury Study Report to Congress. United States Environmental Protection Agency, EPA-452/R-97-003; Office of Air Quality Planning & Standards and Office of Research and Development, : Research Triangle Park, NC, U.S.A., 1997.

(3) Baldi, F.; Bargagli, R. *Mar. Environ. Res.* **1982**, *6*, 69−82.

(4) Baldi, F.; Filippelli, M.; Olson, G. *J. Microb. Ecol.* **1989**, *17*, 263−274.

(5) Guzzi, G.; La Porta, C. A. *Toxicology* **2008**, *244*, 1−12.

(6) Mercury Update: Impact of Fish Advisories. EPA Fact Sheet EPA-823-F-01-011; EPA, Office of Water: Washington, DC, 2001.

(7) Skoog, D. A.; Holler, F. J.; Nieman, T. A. *Principles of Instrumental Analysis*, 5th ed.; Saunders College Publishing: Philadelphia, PA, 1992.

(8) Anderson, K. A. Mercury Analysis in Environmental Samples by Cold Vapor Techniques. In *Encyclopedia of Analytical Chemistry*; Meyes, R. A., Ed.; Wiley: New York, 2006.

(9) Wang, J. *Stripping Analysis: Principles, Instrumentation, and Applications*; VCH Publishers: Deerfield Beach, FL, 1985.

(10) (a) Brulmmer, O.; La Clair, J. J.; Janda, K. D. *Org. Lett.* **1999**, *1*, 415−418. (b) Prodiaaa, L.; Bargossi, C.; Montalti, M.; Zaccheroni, N.; Su, N.; Bradshaw, J. S.; Izatt, R. M.; Savage, P. B. *J. Am. Chem. Soc.* **2000**, *122*, 6769−6770. (c) Nolan, E. M.; Lippard, S. J. *J. Am. Chem. Soc.* **2003**, *125*, 14270−14271. (d) Coronado, E.; Galan-Mascaros, J. R.; Marti-Gastaldo, C.; Palomares, E.; Durrant, J. R.; Vilar, R.; Gratzel, M.; Nazeeruddin, M. K. *J. Am. Chem. Soc.* **2005**, *127*, 12351−12356. (e) Nolan, E. M.; Racine, M. E.; Lippard, S. J. *Inorg. Chem.* **2006**, *45*, 2742−2749. (f) Nolan, E. M.; Lippard, S. J. *J. Am. Chem. Soc.* **2007**, *129*, 5910−5918.

(11) (a) Huang, C.-C.; Chang, H.-T. *Anal. Chem.* **2006**, *78*, 8332−8338. (b) Si, S.; Kotal, A.; Mandal, T. K. *J. Phys. Chem. C* **2007**, *111*, 1248−1255. (c) Yu, C.-J.; Tseng, W.-L. *Langmuir* **2008**, *24*, 12717−12722. (d) Lee, J. S.; Mirkin, C. A. *Anal. Chem.* **2008**, *80*, 6805−6808. (e) Xue, X.; Wang, F.; Liu, X. *J. Am. Chem. Soc.* **2008**, *130*, 3244−3245. (f) Liu, C. W.; Hsieh, Y. T.; Huang, C. C.; Lin, Z. H.; Chang, H. T. *Chem. Commun.* **2008**, 2242−2244.

(12) (a) Chen, B.; Yu, Y.; Zhou, Z.; Zhong, P. *Chem. Lett.* **2004**, *33*, 1608−1609. (b) Zhu, C.; Li, L.; Fang, F.; Chen, J.; Wu, Y. *Chem. Lett.* **2005**, *34*, 898−899.

(13) (a) Liu, X.; Tang, Y.; Wang, L.; Zhang, J.; Song, S.; Fan, C.; Wang, S. *Adv. Mater.* **2007**, *19*, 1471−1474. (b) Ren, X.; Xu, Q.-H. *Langmuir* **2009**, *25*, 29−31.

(14) Chen, P.; He, C. *J. Am. Chem. Soc.* **2004**, *126*, 728−729.

(15) Li, T.; Dong, S.; Wang, E. *Anal. Chem.* **2009**, *81*, 2144−2149.
(16) Dave, N.; Chan, M. Y.; Huang, P.-J. J.; Smith, B. D.; Liu, J. *J. Am. Chem. Soc.* **2010**, *132*, 12668−12673.
(17) Zhang, Y.; Yuan, Q.; Chen, T.; Zhang, X.; Chen, Y.; Tan, W. *Anal. Chem.* **2012**, *84*, 1956−1962.
(18) (a) Chae, M.-Y.; Czarnik, A. W. *J. Am. Chem. Soc.* **1992**, *114*, 9704−9705. (b) Ko, S.-K.; Yang, Y.-K.; Tae, J.; Shin, I. *J. Am. Chem. Soc.* **2006**, *128*, 14150−14155. (c) Jana, A.; Kim, J. S.; Jung, H. S.; Bharadwaj, P. K. *Chem. Commun.* **2009**, 4417−4419. (d) Lee, M. H.; Lee, S. W.; Kim, S. H.; Kang, C.; Kim, J. S. *Org. Lett.* **2009**, *11*, 2101−2104.
(19) Nolan, E. M.; Lippard, S. J. *Chem. Rev.* **2008**, *108*, 3443−3480.
(20) Zhang, J. F.; Kim, J. S. *Anal. Sci.* **2009**, *25*, 1271−1281.
(21) (a) de Silva, A. P.; Gunaratne, H. Q. N.; Gunnlaugsson, T.; Huxley, A. J. M.; McCoy, C. P.; Rademacher, J. T.; Rice, T. E. *Chem. Rev.* **1997**, *97*, 1515−1566. (b) Valeur, B.; Leray, I. *Coord. Chem. Rev.* **2000**, *205*, 3−40. (c) Prodi, L.; Bolletta, F.; Montalti, M.; Zaccheroni, N. *Coord. Chem. Rev.* **2000**, *205*, 59−83.
(22) (a) Métivier, R.; Leray, I.; Valeur, B. *Chem.—Eur. J.* **2004**, *10*, 4480−4490. (b) Chen, Q.-Y.; Chen, C.-F. *Tetrahedron Lett.* **2005**, *46*, 165−168.
(23) (a) Chen, L.; Yang, L.; Li, H.; Gao, Y.; Deng, D.; Wu, Y.; Ma, L. *Inorg. Chem.* **2011**, *50*, 10028−1003. (b) Ma, L.; Li, Y.; Li, L.; Sun, J.; Tian, C.; Wu, Y. *Chem. Commun.* **2008**, 6345−6347. (c) Li, H.; Li, Y.; Dang, Y.; Ma, L.; Wu, Y.; Hou, G.; Wu, L. *Chem. Commun.* **2009**, 4453−4455. (d) Yang, M.-H.; Thirupathi, P.; Lee, K.-H. *Org. Lett.* **2011**, *13*, 5028−5031.
(24) Torrado, A.; Walkup, G. K.; Imperiali, B. *J. Am. Chem. Soc.* **1998**, *120*, 609−610.
(25) (a) Lerchi, M.; Reitter, E.; Simon, W.; Pretsch, E.; Chowdhury, D. A.; Kamata, S. *Anal. Chem.* **1994**, *66*, 1713−1717. (b) Kamata, S.; Bhale, A.; Fukunaga, Y.; Murata, H. *Anal. Chem.* **1988**, *60*, 2464−2467. (c) Kamata, S.; Onoyama, K. *Anal. Chem.* **1991**, *63*, 1295−1298.
(26) Hatai, J.; Pal, S.; Jose, G. P.; Sengupta, T.; Bandyopadhyay, S. *RSC Adv.* **2012**, *2*, 7033−7036.
(27) (a) Shi, W.; Sun, S.; Li, X.; Ma., H. *Inorg. Chem.* **2010**, *49*, 1206−1210. (b) Alfonso, M.; Tarraga, A.; Molina, P. *J. Org. Chem.* **2011**, *76*, 939−947. (c) Mahato, P.; Saha, S.; Suresh, E.; Di Liddo, R.; Parnigotto, P.; Conconi, M. T.; Kesharwani, M. K.; Ganguly, B.; Das, A. *Inorg. Chem.* **2012**, *51*, 1769−1777. (d) Chen, Y.; Wan, L.; Yu, X.; Li, W.; Bian, Y.; Jiang, J. *Org. Lett.* **2011**, *13*, 5774−5777. (e) Pandey, R.; Gupta, R. K.; Shahid, M.; Maiti, B.; Misra, A.; Pandey, D. S. *Inorg. Chem.* **2012**, *51*, 298−311.
(28) Abdo, M. R.; Joseph, P.; Boigegrain, R. A.; Liautard, J. P.; Montero, J. L.; Kohler, S.; Winum, J. Y. *Bioorg. Med. Chem.* **2007**, *15*, 4427−4433.
(29) Ashram, M.; Miller, D. O.; Bridson, J. N.; Georghiou, P. E. *J. Org. Chem.* **1997**, *62*, 6476−6484.
(30) (a) Prodi, L.; Bolletta, F.; Montalti, M.; Zaccheroni, N. *Eur. J. Inorg. Chem.* **1999**, *3*, 455−460. (b) Dhir, A.; Bhalla, V.; Kumar, M. *Org. Lett.* **2008**, *10*, 4891−4894. (c) Chen, L.; Yang, L.; Li, H.; Gao, Y.; Deng, D.; Wu, Y.; Ma, L.-J. *Inorg. Chem.* **2011**, *50*, 10028−10032.
(31) Morgan, M. T.; Bagchi, P.; Fahrni, C. J. *J. Am. Chem. Soc.* **2011**, *133*, 15906−15909.
(32) Nasir, M. S.; Fahrni, C. J.; Suhy, D. A.; Kolodsick, K. J.; Singer, C. P.; O'Halloran, T. V. *J. Biol. Inorg. Chem.* **1999**, *4*, 775−783.
(33) (a) Coronado, E.; Galan-Mascaros, J. R.; Marti-Gastaldo, C.; Palomares, E.; Durrant, J. R.; Vilar, R.; Gratzel, M.; Nazeeruddin, Md. K. *J. Am. Chem. Soc.* **2005**, *127*, 12351−12356. (b) Shunmugam, R.; Gabriel, G. J.; Smith, C. E.; Aamer, K. A.; Tew, G. N. *Chem.—Eur. J.* **2008**, *14*, 3904−3907. (c) Wu, D.; Huang, W.; Lin, Z.; Duan, C.; He, C.; Wu, S.; Wang, D. *Inorg. Chem.* **2008**, *47*, 7190−7201. (d) Das, P.; Ghosh, A.; Bhatt, H.; Das, A. *RSC Adv.* **2012**, *2*, 3714−3721.
(34) (a) Caballero, A.; Martinez, R.; Lloveras, V.; Ratera, I.; Vidal-Gancedo, J.; Wurst, K.; Tarranga, A.; Molina, P.; Veciana, J. *J. Am. Chem. Soc.* **2005**, *127*, 15666−15667. (b) Shortreed, M.; Kopelman, R.; Kuhn, M.; Hoyland, B. *Anal. Chem.* **1996**, *68*, 1414−1418. (c) Lin, W.; Yuan, L.; Cao, Z.; Feng, Y.; Long, L. *Chem.—Eur. J.* **2009**, *15*, 5096−5103.
(35) Zaki, M. T. M.; Esmaile, M. A. *Anal. Lett.* **1997**, *30*, 1579−1590.
(36) http://www.fda.gov/RegulatoryInformation/Legislation/FederalFoodDrugandCosmeticActFDCAct/SignificantAmendmentstotheFDCAct/FDAMA/ucm100218.htm; (accessed May 21, 2012).
(37) Mercury Levels in Commercial Fish and Shellfish (1990−2010) In *National Marine Fisheries Service Survey of Trace Elements in the Fishery Resource*, Report 1978; U.S. Food and Drug Administration: Silver Spring, MD, 2010. (Available on the internet at http://www.fda.gov/food/foodsafety/productspecificinformation/seafood/foodbornepathogenscontaminants/methylmercury/ucm115644.htm (accessed May 21, 2012).